RAA 2019 Vol. **19** No. **7**, 100(8pp) doi: 10.1088/1674–4527/19/7/100

http://www.raa-journal.org *http://iopscience.iop.org/raa*

Research in Astronomy and Astrophysics

The application of co-integration theory in ensemble pulsar timescale algorithm

Feng Gao[1,2,3,4], Ming-Lei Tong[1,2], Yu-Ping Gao[1,2,3], Ting-Gao Yang[1,2] and Cheng-Shi Zhao[1,2]

[1] National Time Service Center, Chinese Academy of Sciences, Xi'an 710600, China; *fengg@xust.edu.cn, mltong@ntsc.ac.cn*
[2] Key Laboratory of Time and Frequency Primary Standards, Chinese Academy of Sciences, Xi'an 710600, China
[3] University of Chinese Academy of Sciences, Beijing 100049, China
[4] Department of Applied Physics, Xi'an University of Science and Technology, Xi'an 710054, China

Received 2018 August 23; accepted 2019 February 11

Abstract Employing multiple pulsars and using an appropriate algorithm to establish ensemble pulsar timescale can reduce the influences of various noises on the long-term stability of pulsar timescale, compared to a single pulsar. However, due to the low timing precision and significant red noises of some pulsars, their participation in the construction of ensemble pulsar timescale is often limited. Inspired by the principle of solving non-stationary sequence modeling using co-integration theory, we put forward an algorithm based on co-integration theory to establish an ensemble pulsar timescale. It is found that this algorithm can effectively suppress some noise sources if a co-integration relationship between different pulsar data exists. Different from the classical weighted average algorithm, the co-integration method provides the chance for a pulsar with significant red noises to be included in the establishment of an ensemble pulsar timescale. Based on data from the North American Nanohertz Observatory for Gravitational Waves (NANOGrav), we found that the co-integration algorithm can successfully reduce several timing noises and improve the long-term stability of the ensemble pulsar timescale.

Key words: pulsars: general — time — methods: analytical

1 INTRODUCTION

Pulsar timing is an effective tool for studying astrophysics and fundamental physics. This includes tests of gravitation, precision constraints on general relativity and especially using arrays of pulsars as detectors for low-frequency gravitational waves (Zhu et al. 2015; Will 2014; Arzoumanian et al. 2015). The basis of pulsar timing is the high-precision timing model, accomplished by the determination of a series of model parameters, such as the spin parameters, astrometric parameters, binary orbit parameters and so on. The errors of the model parameters will affect the timing precision in different ways (Tong et al. 2017). At present, millisecond pulsars (MSPs) have higher stability of rotation and are more widely used in the study of pulsar timescale (Splaver 2004; Verbiest et al. 2009). For example, Hobbs et al. (2012) obtained a preliminary pulsar timescale based on the Parkes Pulsar Timing Array including 19 MSPs observed by the Parkes radio telescope. It was shown that a pulsar timing array allows investigation of "global" phenomena, such as a background of gravitational waves or instabilities in atomic timescales that produce correlated timing residuals in the pulsars of the array. However, there are various physical processes that might be responsible for the accuracy of the pulsar timescale. Timing noise is still not fully understood, but usually refers to unexplained low-frequency features in the timing residuals of pulsars. In the presence of red timing noise, Coles et al. (2011) adopted a transformation based on the Cholesky decomposition of the covariance matrix that whitens both the residuals and timing model, which has sufficient accuracy to optimize the pulsar timing analysis. In addition, using data from multiple pulsars, it is possible to obtain an average pulsar timescale that has stability better than that derived from individual pulsar data (Petit et al. 1993; Rodin 2008; Zhong & Yang 2007; Hobbs et al. 2011).

The purpose of using data from multiple pulsars is to suppress the timing noise intensity of individual pulsars. This approach will open up a new window to improve the

accuracy and long-term stability of pulsar timescales by establishing an ensemble pulsar timescale (EPT). However, similar to the establishment of atomic timescale (AT), the accuracy and long-term stability of EPT depend significantly on information from the timing residuals of the pulsar data involved. The lower the timing noise is, the better the result of EPT that will be obtained, which often limits the participation of a large number of pulsars with significant timing noise. Based on the timing clock model analysis, any clock model can be regarded as a connection between the regression model and time series variables. Whether establishing a good pulsar timescale or forecasting it, the clock difference series should be stationary. Only in this way can we ensure that some statistical parameters in the selection and examination of the model, such as coefficient of determination R^2 and T statistics, have a standard normal distribution, and therefore, the statistics are reliable. Otherwise, all of the above inferences can easily produce a spurious regression.

In the field of economics, in order to avoid spurious regression of non-stationary series, Engle & Granger (1987) proposed the co-integration theory that provides another way for the modeling of non-stationary series. For example, although some economic variables themselves are non-stationary series, a linear combination of them is likely to be stationary. This combination process is known as the co-integration equation, and it can explain the long-term equilibrium relationship between different variables. In principle, pulsars with significant timing noise show non-stationary characteristics of timing residuals. If the linear combination of pulsar timing residuals is a stationary series, they are also co-integrable. According to the above ideas, an algorithm based on co-integration theory to establish EPT is proposed in this paper, which mainly uses pulsars with significant timing noise, and the results show that the algorithm can successfully reduce several timing noises and significantly improve the long-term frequency stability of EPT. Co-integration is a powerful method, because it not only allows us to characterize the equilibrium relationship between two or more non-stationary series, but also will provide better guidance in studying the establishment of EPT in future.

2 CO-INTEGRATION AND METHOD

In the process of regression analysis for most non-stationary time series, the difference method is usually used to eliminate the non-stationary trend term in the series, so that the series can be modeled after it is stationary. However, the series themselves after difference calculation often are limited in terms of the scope of the problem discussed and make the reconstructed model difficult to explain. Co-integration theory has greatly alleviated the difficulty of non-stationary series in modeling. Co-integration theory is proposed for integration. A series with no deterministic component which has a stationary, invertible, autoregressive moving average (ARMA) representation after difference d times is said to be integrable of order d, denoted as $Y_t \sim I(d)$. Obviously, for $d = 0$, Y_t will be stationary.

Table 1 Basic Parameters for Seven Pulsars

Pulsar name	P (ms)	Number of TOAs	RMS (μs)	Span (yr)
J0030+0451	4.87	2468	0.723	8.8
J0613–0200	3.06	7651	0.592	8.6
J1012+5307	5.26	11 995	1.197	9.2
J1643–1224	4.62	7119	2.057	9.0
B1855+09	5.36	4071	1.339	8.9
J1910+1256	4.98	2690	1.449	8.8
B1937+21	1.56	9966	1.549	9.1

Co-integration theory can be understood in that there may be a long-term equilibrium relationship between several time series with the same order of integration, and one kind of linear combination of them has a lower order of integration. To formalize these ideas, the following definition adopted from Engle and Granger is introduced: (i) if all components of Y_t are $I(d)$; (ii) there exists a vector α ($\neq 0$) so that $\alpha^{'} Y_t \sim I(d-b)$, $d \geq b \geq 0$. The components of the vector Y_t are said to be co-integrable of order d, b, denoted as $Y_t \sim CI(d-b)$, and the vector α is called the co-integrating vector.

In general, there are two main methods to examine the co-integration, including the Engle-Granger (EG) two-step method and Johansen-Juselius (JJ) multivariate maximum likelihood method (Engle & Granger 1987; Johansen 1995). The major difference between the above methods is that the EG two-step method adopts the technique of solving linear equations, while the JJ test uses the multivariate equation technique. In this paper, the EG method is adopted to assess the null hypothesis of no co-integration among the time series in Y_t. Detailed test steps can be seen in Engle & Granger (1987).

3 EPT ALGORITHM BASED ON CO-INTEGRATION THEORY

In pulsar timing, the timing residuals are the differences between the observed times of arrival (TOAs) and the ones predicted by the timing model, i.e., the difference between two timescales, AT and PT. Here, PT stands for the pulsar timescale. However, in practical data processing, the TOAs recorded in terms of AT should be transformed to Barycentric Coordinate Time (TCB), and PT is predicted at Solar System Barycenter (SSB) by the pulsar timing model. Hence, for a given pulsar i, the residuals are de-

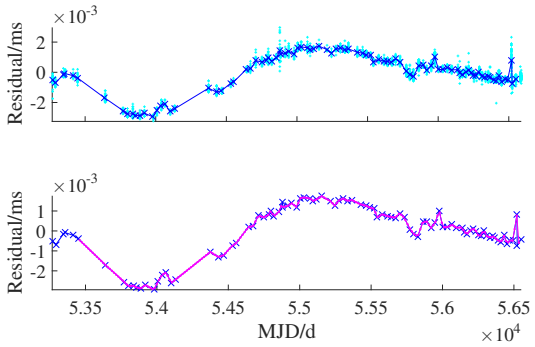

Fig. 1 The raw timing residuals vs. two-step preprocessing residuals for pulsar B1937+21 (the *cyan* and *blue* represent the raw residuals vs. the averaged residuals in panel a), and *blue* and *magenta* stand for the averaged residuals vs. linear interpolation residuals in panel b).

noted as

$$\mathrm{Res}_i = AT - PT_i\,, \tag{1}$$

where Res_i is a timing residual; AT is reference atomic time; PT_i is pulsar time for a given pulsar i. The EPT (Petit & Tavella 1996) established by multiple pulsars (i =1, 2, $\cdots$, n) can be defined as

$$AT - EPT = \sum_{i=1}^{n} \omega_i (AT - PT_i)\,, \tag{2}$$

where ω_i is the relative weight assigned to pulsar i. Because we adopted the EG test to analyze pulsar data in this paper, and hence assume that for two known pulsars whose timing residuals are $\mathrm{Res}_i \sim I(1)$ when they are co-integrated, the co-integrated regression equation for both sets of timing residuals can be expressed as

$$\mathrm{Res}_1 = \alpha + \beta \mathrm{Res}_2 + \hat{\varepsilon}\,, \tag{3}$$

where α and β represent regression coefficients; $\hat{\varepsilon}$ is the model residuals, and $\hat{\varepsilon} \sim I(0)$. According to Equations (1)–(3) we obtain

$$\begin{cases} \omega_1 = \frac{1}{1-\beta}, \\ \omega_2 = \frac{-\beta}{1-\beta}, \\ \mathrm{Res}_{\mathrm{ept}} = \frac{\hat{\varepsilon}+\alpha}{1-\beta}, \end{cases} \tag{4}$$

where $\mathrm{Res}_{\mathrm{ept}}$ signifies the timing residuals of EPT. This can be regarded as a transformation from $\hat{\varepsilon}$ by shift factor α and scale factor $(1-\beta)$, and both α and $(1-\beta)$ are constant coefficients, which will not affect the order of integration, so $\mathrm{Res}_{\mathrm{ept}} \sim I(0)$.

4 OBSERVATIONAL DATA

4.1 NANOGrav Timing Observations

We used pulsar timing data from the North American Nanohertz Observatory for Gravitational Waves (NANOGrav) nine-year data set described in The NANOGrav Collaboration et al. (2015) (hereafter NG9) for our analysis. NG9 contain 37 MSPs observed at the Green Bank Telescope (GBT) and Arecibo Observatory (AO). Each telescope is equipped with two generations of backends, with more recent backends processing up to an order of magnitude larger bandwidth for improving pulse sensitivity. Polarization calibration and radio frequency interference (RFI) excision algorithms were applied to the raw data profiles using the PSRCHIVE (Hotan et al. 2004; van Straten et al. 2012) software package when pulse profiles were folded and de-dispersed using an initial timing model. After calibration, known RFI signals were excised and the final pulse profiles used to generate TOAs were fully time averaged with some frequency averaging to build pulse signal-to-noise ratio (S/N). See NG9 for more details on the data processing method. Because the purpose of this article is to improve the long-term frequency stability of EPT consisting mostly of pulsars with significant timing noise, and the stability of a pulsar timescale is related to the timing span, in this paper the requirement for selecting pulsars from NG9 is that both the sampling time span is longer than 8 yr and the detection is obvious at low frequency, taking the form of "red" timing noise in timing residuals for the pulsars. We identified seven pulsars that met these criteria; see the basic parameters for these seven pulsars in Table 1.

4.2 Data Preprocessing

NG9 contained all TOAs and timing solutions for 37 pulsars. Each pulsar was observed at each epoch with at least two receivers. At GBT, the 820 and 1400 MHz bands were used, and at AO, the 430 and 1400 MHz or 1400 and 2300 MHz bands were used. We note that the frequency-dependent profile shape changes across the entire observing band can be significant for some sources over the full band (Pennucci et al. 2014), and we wish to maintain homogeneity in the inferred timing data from our pulsars, so we only analyze timing residuals associated with 1400 MHz. In addition, data from pulsar B1937+21 were just from GBT. We use the unit root test with significance level 0.01 to analyze residual data for seven pulsars. The results show that they all seem to be stationary, Res∼I(0). This may be due to mostly MSPs in NG9 having a higher stability of rotation, the dispersion of timing residuals being dominated by white noise or red noise being drowned out by the white one within a shorter observation span. Hence, we choose pulsar data with significant red noise and further reduce the white noise intensity in the timing residuals in some way that can make the processed data meet the condition of being non-stationary, Res∼I(1),

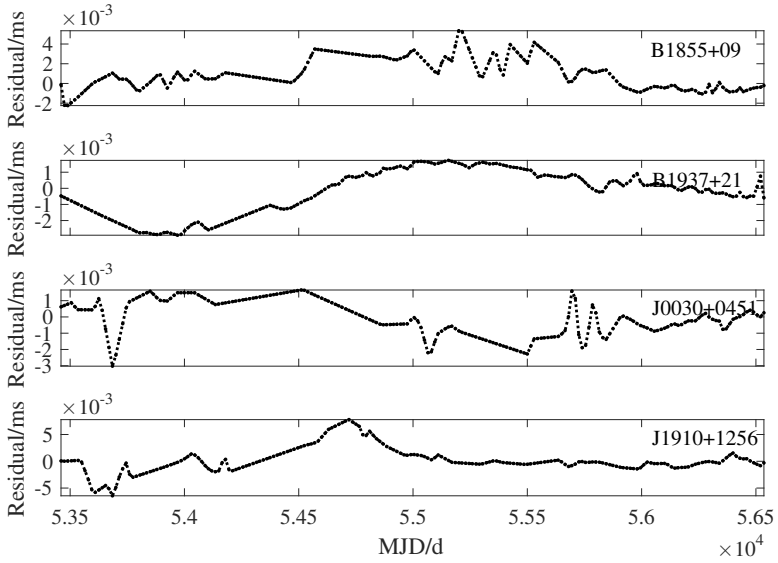

Fig. 2 The timing residuals for four known pulsars B1855+09, B1937+21, J0030+0451 and J1910+1256, from top to bottom respectively.

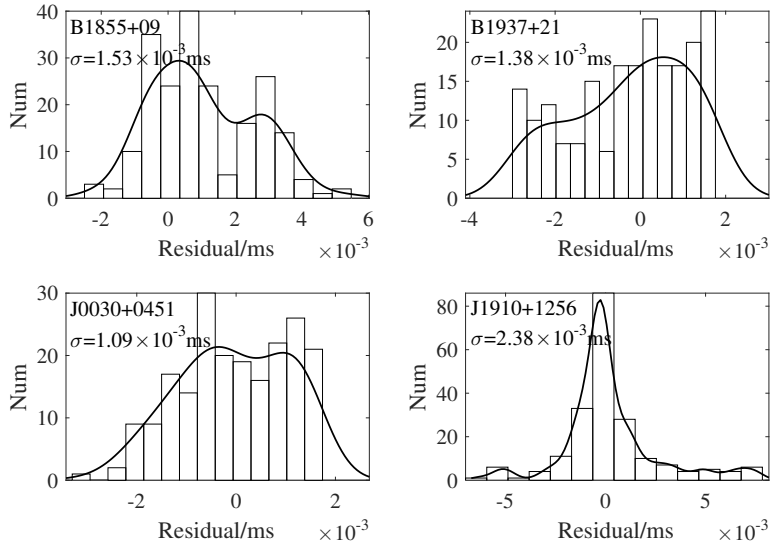

Fig. 3 The histograms of timing residual distributions for four known pulsars B1855+09, B1937+21, J0030+045 and J1910+1256. The *solid line* is the fitting curve for each residual distribution. The values of standard deviation (σ) for the four residual distributions are also given.

which is equivalent to just retaining the red noise component in the original data. Besides, pulsar timing observations are usually irregular and the associated sampling rate is much lower than that compared to an atomic clock. Thus, a simple method will be adopted to reduce the intensity of white noise and make the two columns of data involved in the co-integration test correspond to each other.

For long-term pulsar timing studies, it becomes useful to visually inspect timing residuals that have been averaged in order to look for long term trends or biases. The following details on data preprocessing will be illustrated with one pulsar, i.e., J1937+21: Firstly, we construct daily averaged residuals, with each residual value being equal to the average of all raw residuals within one day. This process is similar to comparing pulsar time with an atomic clock once a day. Subsequently, the data are linearly interpolated and sampled at intervals of about 15 days to obtain equally distributed data. The purpose of the above two-step process is to reduce the white noise intensity and further help analyze whether the low-frequency noise in residu-

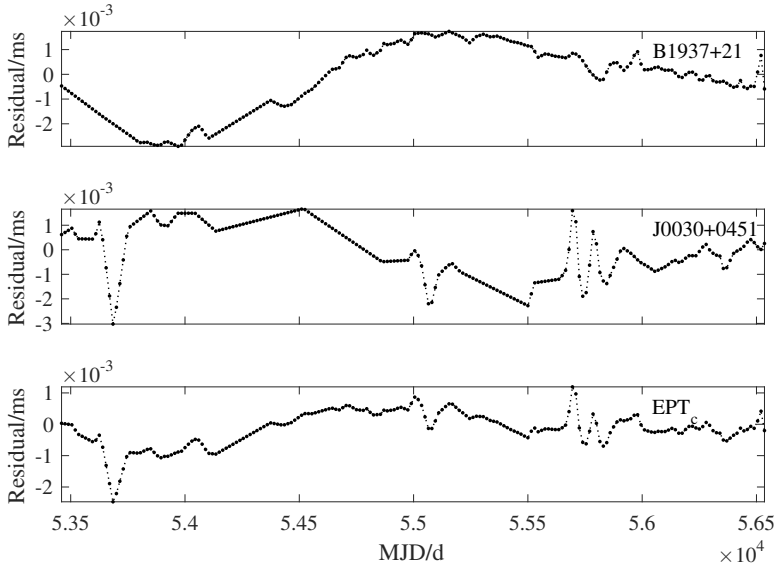

Fig. 4 The timing residuals for two known pulsars B1937+21 and J0030+0451, and for $\mathrm{EPT_c}$, from top to bottom respectively.

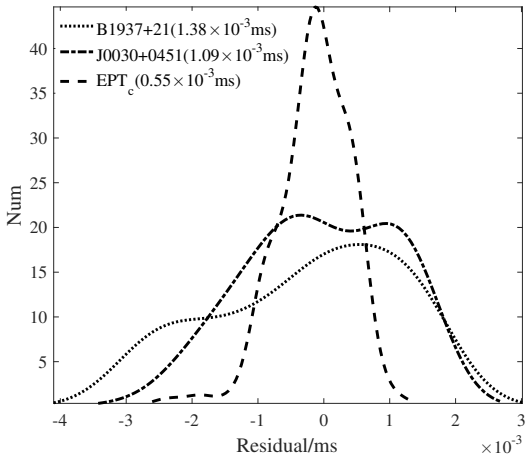

Fig. 5 The fitting curves of timing residual distributions for two known pulsars (*dotted line* for B1937+21 and *dash-dotted line* for J0030+0451) and for EPT (*dashed line* for $\mathrm{EPT_c}$). The values of standard deviation for the three residual distributions are also given in parentheses.

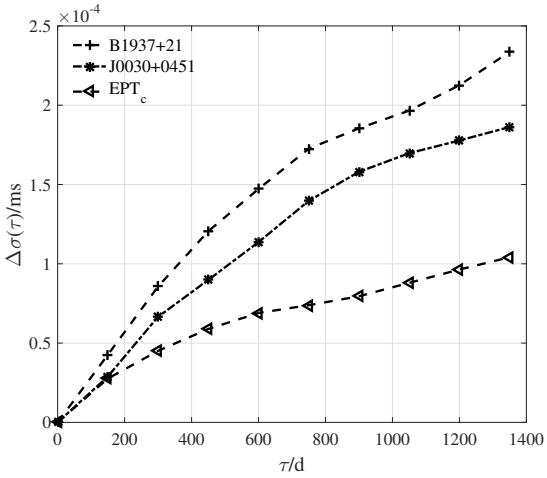

Fig. 6 The standard deviation increment of timing residuals vs. timing span for two known pulsars (*plus signs* for B1937+21 and *asterisks* for J0030+0451) and for EPT (left-pointing triangles for $\mathrm{EPT_c}$).

als for different pulsars has a co-integration relationship with each other. Other methods that only discuss the reduction of white noise intensity will be given in future work. The original timing residual distribution vs. two-step preprocessing residual data are shown in Figure 1. Similarly, timing residuals from six other known pulsars are also regularly processed.

5 RESULTS AND ANALYSIS

According to the mathematical model of co-integration theory in Section 3, it is necessary to examine the integrated order of the time series to determine whether there are co-integrated relationships. In this paper, the EG method was adopted to examine timing residuals of all pulsars after preprocessing data. We found that pulsars B1855+09, B1937+21, J0030+0451 and J1910+1256 were integrated of order 1, denoted as $I(1)$, and others were $I(0)$. These results may be due to the intensity of red noise in residuals of pulsars J0613-0200, J1012+5307 and J1643-1224 being relatively weak. After data preprocessing, timing residuals still show some "quasi-stationary" features. In order to search for pulsars with a co-integration relationship by using only the EG two-step method, we apply further analysis to pulsars B1855+09, B1937+21, J0030+0451 and J1910+1256.

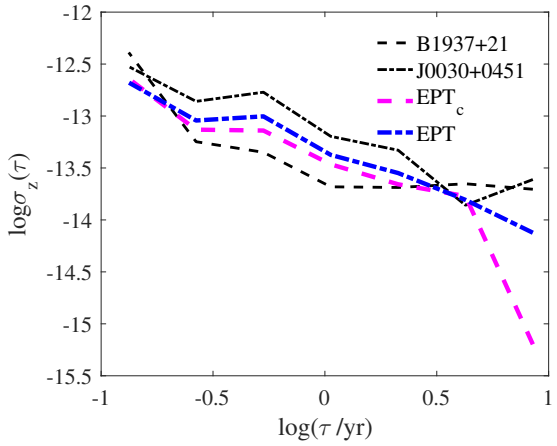

Fig. 7 Stability of pulsar timescale for two known pulsars (*dashed line* for B1937+21 and *dash-dotted line* for J0030+0451) and for EPT calculated by different algorithms (*magenta dashed line* for $\mathrm{EPT_c}$ and *blue dash-dotted line* for EPT) (*Color version is online*).

The timing residuals of pulsars B1855+09, B1937+21, J0030+0451 and J1910+1256 are depicted in Figure 2, and the histograms of residual distributions can be seen in Figure 3. In Figure 2, the timing residual distributions for all pulsars show an obvious irregular low-frequency trend, and histograms of residual distributions are significantly different from the normal distribution in Figure 3. All of these indicate that the timing residuals for four known pulsars have a common feature of instability, which is consistent with the case where the integrated order of residuals is denoted as $I(1)$. In addition, by comparing the residual distributions and standard deviations of the residuals, we find there are significant differences in the different sets of pulsar data. These differences are not only apparent in the trend of the associated residual distribution, but also in the shape of the fitting curve. These are related to the fact that every pulsar data set is affected by different sources of noise.

Next, according to Equation (3) in Section 3, we should further examine the linear combination for residuals from two random pulsars (for example pulsars A and B) with associated $I(1)$. If $\hat{\varepsilon}$ is integrated of order 0, then pulsars A and B are co-integrable. We found that only the linear combination of pulsars B1937+21 and J0030+0451 meets the condition that $\hat{\varepsilon}$ is given by $I(0)$, indicating that pulsars B1937+21 and J0030+0451 are co-integrable. The timing residuals of the EPT established by pulsars B1937+21 and J0030+0451 can be obtained according to Equation (4) in Section 3 and called $\mathrm{EPT_c}$. In order to measure the degree of stability of the associated residuals, first of all, we compared both residual distributions and residual histograms for pulsars B1937+21, J0030+0451 and $\mathrm{EPT_c}$ in Figures 4 and 5.

In Figure 4, we can see that the amplitude fluctuations of residuals for pulsars B1937+0451 and J0030+0451 are stronger and have obvious low-frequency features, but the residuals for $\mathrm{EPT_c}$ are characterized by normalization, simplicity, significant reduction of non-stationary process, etc. The ranges of residual amplitude variation for pulsars B1937+21 and J0030+0451, and $\mathrm{EPT_c}$ are $(-2.91, +1.74)$ μs, $(-3.03, +1.66)$ μs and $(-2.47, +1.19)$ μs, respectively. The standard deviation for $\mathrm{EPT_c}$ is smallest. In addition, the shape of the fitting curve for $\mathrm{EPT_c}$ in Figure 5 is also closer to a normal distribution than those of pulsars B1855+09 and J0030+0451. The above aspects all indicate that the degree of stability for $\mathrm{EPT_c}$ has been greatly improved.

5.1 Variance Analysis

The dispersion of pulsar timing residuals can be divided into white and red noise. White noise mainly comes from random errors in the process of timing observation, while red noise is a kind of signal having strong intensity at lower frequencies, giving it a power-law spectral density. We can define the dispersion of residual as σ_{RMS}, while white noise is denoted σ_{W} and red noise is labeled σ_{TN} (Yang et al. 2014; Gao et al. 2018). In theory, their relations are as follows

$$\sigma_{\mathrm{RMS}}{}^2 = \sigma_{\mathrm{W}}{}^2 + \sigma_{\mathrm{TN}}{}^2 , \tag{5}$$

where if the ratio of σ_{RMS} to σ_{W} is close to 1, it indicates that the dispersion of residuals is mainly affected by white noise and the data are stationary. If the value of $\sigma_{\mathrm{RMS}}/\sigma_{\mathrm{W}}$ is much higher than 1, it indicates that there is a significant red noise component within the timing residuals. Generally, the effect of red noise on dispersion of residuals changes with increasing observing span. To reflect this change, Gao et al. (2018); Lam et al. (2017) used variance increment to show an important contribution of red noise to residual fluctuation. Considering that the dimension of standard deviation is consistent with the magnitude of data, it is more obvious when describing data dispersion, and the variance and standard deviation can be easily converted to each other. As defined by Gao et al. (2018), the standard deviation increment is written as follows

$$\Delta\sigma(\tau) = \langle \mathrm{Var}(X(t+\tau))^{1/2} - \mathrm{Var}(X(t))^{1/2} \rangle , \tag{6}$$

where t stands for timing span, $\mathrm{Var}(X(t))$ represents the variance of the data in t and τ is the increment of timing span. In theory, for data with significant systematic fluctuations, the standard deviation increment will change with an increase of τ. In this paper, we take the pulsar B1937+21 as an example to illustrate how to choose the values for parameters t and τ. After data preprocessing,

there are 206 points corresponding to residuals for pulsar B1937+21 in 8.4 yr, and the interval between two points is approximately 15 days. To take t as the interval span of ten adjacent points, for τ =0, 10, 20, $\cdots$, sequentially add an interval span of ten points. Meanwhile, in order to avoid introducing statistical error, the standard deviation increment in (6) is averaged. The timing span is divided into at least two segments, so the maximum span of τ is nearly half of 8.4 yr. Similarly, pulsar J0030+0451 and $\mathrm{EPT_c}$ are processed in the same way. The relations between standard deviation increment and timing span for three pulsars are shown in Figure 6.

As visible in Figure 6, the values of $\Delta\sigma(\tau)$ for pulsars B1937+21 and J0030+0451 increase rapidly with the change of τ, while the $\Delta\sigma(\tau)$ for $\mathrm{EPT_c}$ changes slowly. This is because red noise in the residuals of pulsars B1937+21 and J0030+0451 is obvious. Along with the timing span increase, strong red noise becomes an important factor for the dispersion of residuals from a pulsar. This is consistent with the fact that the integrated order of two pulsars is 1. It can also be explained in that the linear combination of pulsar residuals which are co-integrable is a stationary series by $\mathrm{EPT_c}$.

5.2 $\sigma_z(\tau)$ Methods

Using the exceptionally stable rotation of MSPs to generate a timescale needs a reliable statistical measure for studying the physics of pulsar rotation and comparing pulsar stabilities with those of terrestrial clocks. Clock data are commonly analyzed using a statistic called $\sigma_y(\tau)$, the square root of the "Allan variance" (Allan 1966), which can be computed from second differences of a table of clock offset measurements. $\sigma_y(\tau)$ is ideally suited for analyzing AT which have very small frequency drift rates. However, for most pulsar timing data, the lowest-order deviations are related to the $third$ difference, which remains in a pulsar timing series after the phase, frequency, spin-down rate and astrometric parameters have been determined by comparison with terrestrial time, and their effects are removed. Following Taylor (1991), the $\sigma_z(\tau)$ statistic, defined in terms of third-order polynomials fitted to sequences of measured time offsets, is suggested for studying the pulsar timing data. Since it is more sensitive to redder noise than other commonly used measures, and is suited for comparing pulsar stabilities with those of other timescales. In this paper, we utilize an improved $\sigma_z(\tau)$ proposed by Matsakis et al. (1997), which is a good statistic for the analysis of low-frequency-dominated red noise of pulsar timing residuals. To find $\sigma_z(\tau)$, divide the data into subsequences and fit a cubic function to the data in each subsequence by minimizing the weighted sum of squared differences

$$R^2 = \sum_{i=1}^{N_m} \left[x(t_i) - \frac{X(t_i)}{\sigma_i} \right]^2 = \min\,, \tag{7}$$

then set

$$\sigma_z(\tau) = \frac{\tau^2}{2\sqrt{5}} \langle c_3^2 \rangle^{1/2}\,, \tag{8}$$

where angled brackets denote averaging over the subsequences, weighted by the inverse squares of the formal errors in c_3. The detailed recipe for the computation of $\sigma_z(\tau)$ can be referenced in Matsakis et al. (1997).

In Figure 7, we present values of $\sigma_z(\tau)$ for both pulsars B1937+0451 and J0030+0451, and EPT_c, defined as the weighted root-mean-square of the coefficients of the cubic terms fitted over intervals of length τ. For comparison, another EPT calculated by the traditional classical weighted average algorithm is given in Figure 7. The weights ω_i are inversely proportional to the variance of two pulsars 1937+21 and J0030+0451, respectively. Because $\sigma_z^2(\tau)$ can be easy to describe by a power law, if white noise is dominant in the time series, the slope of the log-log graph is close to –1.5 for all four time series, showing that at least up to intervals for τ of several years, as expected for residuals dominated by uncorrelated measurement errors. By contrast, when the red noise is dominant, the tail of the curve will gradually become an upward trend, which is interpreted as the influence of low-frequency noise on frequency stability. For both pulsars B1937+21 and J0030+0451, the curves display a tail-upward trend, while the curves of both $\mathrm{EPT_c}$ and EPT exhibit a downward trend as a whole. This indicates that the timing residuals for two pulsars B1937+21 and J0030+0451 are dominated by low-frequency noise believed to be intrinsic to the pulsars. It is noted that the stability of pulsar timescale for pulsar J0030+0451 at $\log\tau$ $\sim$0.6 is more stable than that for $\mathrm{EPT_c}$. This anomaly should be induced by the increasing errors of σ_z for larger intervals of length τ because of the decreasing number of sequences.

The level of long-term frequency stability plays an important role in the study of pulsar timescales. Figure 7 demonstrates that the value of $\sigma_z(\tau)$ for the two pulsars B1937+0451 and J0030+0451 and for EPT calculated by the different algorithm $\mathrm{EPT_c}$ and EPT in the span 8.4 yr are $10^{-13.70}$, $10^{-13.61}$, $10^{-15.20}$ and $10^{14.12}$, respectively. The long-term frequency stability of $\mathrm{EPT_c}$ is nearly one order of magnitude higher than those of the two pulsars, B1937+0451 and J0030+0451. In addition, one can note that the stability of $\mathrm{EPT_c}$ is better than EPT as a whole in Figure 7. The above analysis indicates that the long-term frequency stability level of a pulsar can be significantly improved within a limited observation span when combining pulsar data with the co-integration relation to establish EPT. One thing to keep in mind is that these stabilities

of pulsars in Figure 7 are not further compared with other pulsar data that have weak red noise and AT at different stations. This is because there are many factors influencing the stabilities of different timescales. In this paper, we only demonstrate that the method to establish EPT based on combining the pulsar data with the co-integration relation is reliable and feasible. Further research will be carried out in follow-up work.

6 DISCUSSION AND CONCLUSIONS

It should be noted that it is necessary to satisfy a strict constraint condition to establish EPT based on the co-integration theory: the timing residuals of pulsars are co-integrable. The combination of timing residuals with the co-integration relation can only reduce the number of integrated order, and in this way it can obviously reduce the timing noise intensity of EPT and improve its long-term frequency stability. This constraint condition means that the following problems may be encountered in practical application: (1) In a short span, the red noise in residuals of MSPs is not dominant or cannot be measured, and residual data show "quasi-stationary" characteristics, which will limit the application of methods in data. (2) At present, the low-frequency timing noise of most pulsar data is irregular, which means that the co-integration relation between pulsars may be negatively affected by the increase or decrease of the data span. This may lead to segmented co-integration. In addition, we only use the EG (Engle & Granger 1987) two-step test to discuss and establish the EPT algorithm based on two pulsars in this paper. If data from multiple pulsars are regarded as multivariate variables, and the co-integration relation between them is tested by using the JJ (Johansen 1995) method, the application of co-integration theory in the algorithm of EPT can be further extended.

Based on the co-integration theory, an algorithm to establish EPT by using pulsar data with significant timing noise is proposed in this paper. This algorithm can successfully reduce several types of timing noise and improve the long-term stability of the associated pulsar timescale. Compared to the optimal weighting method (Rodin 2008) and the global fitting method (Hobbs et al. 2012), our co-integration method is similar to the traditional classical weighted average method but with a new way of choosing weights. However, different from the traditional classical weighted average algorithm, this algorithm can effectively suppress some noise sources if there is a co-integration relationship between different pulsar data, and provides the chances of a pulsar with significant red noises to be included in the establishment of EPT.

Acknowledgements This work was funded by the National Natural Science Foundation of China (Grant Nos. 11373028, U1531112, 91736207, 11873050, 11873049 and U1831130), the A Project of the Young Scholar of the "West Light" of the Chinese Academy of Sciences (XAB2015A06) and the Cultivation Fund of Xi'an University of Science and Technology (No. 201707).

References

Allan, D. W. 1966, IEEE Proceedings, 54, 211
Arzoumanian, Z., Brazier, A., Burke-Spolaor, S., et al. 2015, ApJ, 810, 150
Coles, W., Hobbs, G., Champion, D. J., et al. 2011, MNRAS, 418, 561
Engle, R. F., & Granger, C. W. J. 1987, Econometrica, 55, 251
Gao, F., Gao, Y.-P., Tong, M.-L., et al. 2018, Sci Sin-Phys Mech Astron, 48, 059501 (in Chinese)
Hobbs, G., Coles, W., Manchester, R., & Chen, D. 2011, in Journées Systèmes de Référence Spatio-temporels 2010, ed. N. Capitaine, 237
Hobbs, G., Coles, W., Manchester, R. N., et al. 2012, MNRAS, 427, 2780
Hotan, A. W., van Straten, W., & Manchester, R. N. 2004, PASA, 21, 302
Johansen, S. 1995, Likelihoodbased Inference in Cointegrated Vector Autoregressive Models (Oxford: Oxford Univ. Press)
Lam, M. T., Cordes, J. M., Chatterjee, S., et al. 2017, ApJ, 834, 35
Matsakis, D. N., Taylor, J. H., & Eubanks, T. M. 1997, A&A, 326, 924
Pennucci, T. T., Demorest, P. B., & Ransom, S. M. 2014, ApJ, 790, 93
Petit, G., Thomas, C., & Tavella, P. 1993, in 24th Annual Precise Time and Time Interval (PTTI) Applications and Planning Meeting, ed. R. L. Sydnor, 73
Petit, G., & Tavella, P. 1996, A&A, 308, 290
Rodin, A. E. 2008, MNRAS, 387, 1583
Splaver, E. M. 2004, Long-term Timing of Millisecond Pulsars, PhD thesis, Princeton University
Taylor, Jr., J. H. 1991, IEEE Proceedings, 79, 1054
The NANOGrav Collaboration, Arzoumanian, Z., Brazier, A., et al. 2015, ApJ, 813, 65
Tong, M.-L., Yang, T.-G., Zhao, C.-S., et al. 2017, Sci Sin-Phys Mech Astron, 44, 099503 (in Chinese)
van Straten, W., Demorest, P., & Oslowski, S. 2012, Astronomical Research and Technology, 9, 237
Verbiest, J. P. W., Bailes, M., Coles, W. A., et al. 2009, MNRAS, 400, 951
Will, C. M. 2014, Living Reviews in Relativity, 17, 4
Yang, T.-G., Tong, M.-L., Gao, Y.-P. 2014, J Time Freq, 37, 80 (in Chinese)
Zhong, C.-X., & Yang, T.-G. 2007, Acta Phys. Sin. 56, 6157 (in Chinese)
Zhu, W. W., Stairs, I. H., Demorest, P. B., et al. 2015, ApJ, 809, 41